Reflectivity and Elastic Modulus of Nano-Aluminum Films on Silicon Crystal Substrates

by

Raed Alharbi

A thesis
presented to the University of Waterloo
in fulfillment of the
thesis requirement for the degree of
Master of Applied Science
in
Mechanical Engineering

Waterloo, Ontario, Canada, 2014

Author's Declaration

I hereby declare that I am the sole author of this thesis. This is a true copy of the thesis, including any required final revisions, as accepted by my examiners.

I understand that my thesis may be made electronically available to the public.

Abstract

In this work, effect of film thickness on optical reflection and elastic modulus of the metal film at very low size was studied. We choose Aluminum as a reflective surface where it mostly used as a typical material for micro mirror device due to its high reflectivity. The effect of film thickness on the reflectivity had been performed at the range of 400-700 nm wavelengths for thin film thicknesses between 10 - 125 nm. The mirror fabricated by depositing the Al films on single crystal silicon (100) substrates using E beam evaporation deposition machine to get optimum flatness that is desired in the mirror fabrication. After that, reflection of the mirrors was measured using UV 2200 Spectrophotometer. Reflection also simulated using a powerful simulation tool, Opti-FDTD finite element package and the results were compared. Both of grain size and surface roughness of the films were measured using Scanning Electron Microscopy (SEM) and Atomic Force Microscope (AFM, tapping mode), respectively, to study the reason of deviation between the simulated and experimental results of reflection. In addition, elastic modulus of the films was measured using nanoindentation method using AFM (Contact mode) and the results compared to bulk value.

General increasing in the reflection as the film thickness increased and decrease in the reflection as the wavelength increased was observed. At lower film thickness, 10 nm, the film had very low reflection compared to other films. After comparison between the experiments and the simulation results, it appears that deviation between them increase as the film thickness decrease and the topography of the metal surface is the reason behind that. Finally, elastic modulus of the films were determined and it shows that there is decrease in the films modulus and sharp decrease at 50 nm film thick.

Acknowledgements

After a great thanks to God, for this completion, I want to thank my parents, in Saudi Arabia, for their help and support.

Highly Appreciation to my supervisors Prof. Mustafa Yavuz and Prof. Eihab Abdullrahman for their support and help during my master work.

Also, thanks for Prof. Yu Sun at University of Toronto for his support using the AFM in his lab.

Also, thanks for Prof. Ting Tsui in Chemistry department for his support using the SEM in his lab.

Thanks for Mehrdad for his help in sample preparation and reflection simulation.

Thanks also, for people who helped me on training on equipments I used in my work: Minoli (Spectrometer, G2N lab), Greame (AFM, G2N lab), Joe (SEM, Prof. Ting's lab), and Haijiao (AFM, Prof. Sun's lab)

I am very thankful to my country, Saudi Arabia, for supporting me during Master

Thanks for my wife, Hind, for her support during living in Canada.

Lastly, I am thankful to my family in Saudi Arabia.

Dedication

To my father : Abdullah

To my mother : Bakita

To my wife: Hind

To My University: Taibah University

Table of Contents

List of Tables

List of Figures

Chapter 1

Introduction

1.1 Thin Film Reflectance

Aluminum is one of the high reflective materials in visible spectrum of light. It is mostly used in optical devices such as micromirror applications in display devices. In the micromirror, aluminum is used as a reflective plate that deposited on such substrate such as silicon due to a very small thickness used where it's in micro or nano range. Thickness of the film is one of the essential parameters affect the reflectivity of the mirror. Hass and Waylonis reported the reflection of aluminum at 300 nm wavelength for different film thickness which shows that as the thickness increase the reflection increase and vice versa[17]. From the quantum point of view and according to Bragg law, plane distance is one of the parameters that lead to constructive or destructive waves after reflection which in constructive case the reflection will be stronger [25]. Similar to that but, in the case of thin film interference we deal with the thickness of the film. Another point that play a role in the reflection in the case of thin film interference is the angle of incident which is affect the phase change and accordingly affect the reflection. Using a Bragg law again, the length of the light travel through the film affects the case of interference. If the total length of the distance travelled by the light in the film is an integral multiple of the wavelength, then the case of the interference is constructive and the reflection is higher than in opposite case [25]. Figure 1.1 shows the case of the interference of the thin film and equation 1.1 describe the condition of the interference

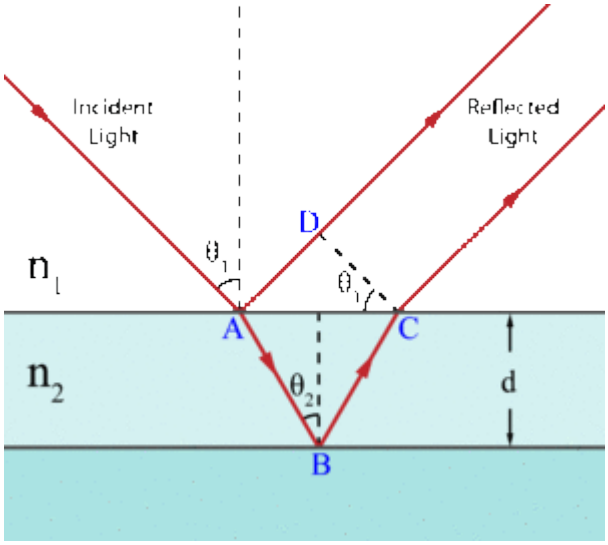

Figure 1.1: Optical path difference for the reflected light from upper and lower thin film boundaries [25]

$$2n_2 dcos\left(\Theta_2\right) = m\lambda \tag{1.1}$$

Different works were done to calculate the optical properties of different materials. Mihailo and Alexander calculate the reflection coefficient of the laser light of wavelengths (0.22 um - 200 um) from the surface of aluminum using the Lorentz-Drude model and they found that the reflection is ranging from 0.90 up to 0.99 depending on the wavelength and their values matched the literature results [27]. In addition to that, Jaeckin et al, measured the surface reflectivity of the aluminum of 2 um film thickness at normal incident and they found that the reflection is equal to 0.66 [21]. In their work they found that the reflection is decrease due to some fabrication issues such as etching and made a drop in the reflectivity value from 0.83 to 0.66. Any material has a specific penetration depth and its varying depending on the frequency of the wave and can be calculated using skin depth effect using equation 1.2.

$$\delta = 503\sqrt{\frac{\rho}{\mu_r f}} \tag{1.2}$$

where: δ = the skin depth in metre, μ_r = the relative permeability of the medium, ρ = the resistivity of the medium, f = the frequency of the wave in Hz.

Also, roughness of the film affects the reflection where high surface roughness results in low reflection. [2]. For evaporated aluminum film on silicon substrate, reported by Kirill [8], the surface roughness decrease as the deposition rate decrease, so, the deposition rate should be considered during fabrication. Grain size also affect the reflection of material where as the grain size decrease the reflection decrease due to increase in the scattering of the reflected light in the case of larger number of grain boundaries.

1.2 Grain Size of Thin Film

Grain boundary is a one of the material defects. It is a planner defect that separates two or more grains or crystallites in a polycrystaline material. It is resulted from uneven growth during crystallization. The grain boundaries are the where the grains are met and they are the transition region between the neighbouring crystals. Grain size can be number of nanometers up to some millimeters.[13]

Grain size has different effects on mechanical properties of material. One of the mechanical properties is the strength of material that is enhanced by increase the grain size of the material. James et al. [32] tested the strength of two thin aluminum fibers with 35 and 100 nm grain size by pulling them in a micro-tensile tester. They found that the sample with larger grain size led to greater yield and tensile strength and smaller strains to failure. They also noticed that both samples had mechanical strength 3-6 times larger than the strength of bulk aluminum.

Film thickness affects the value of grain size where as the film thickness decrease the grain size decrease, too. Diego et al. [11] studied the effect of film thickness on grain size for aluminum thin films deposited on glass substrate and came up with results as shown in figure 1.2. They found that there is a linear dependency between the grain size and the film thickness and the grain size is not constant nor equal to film thickness. Even they tested different samples deposited with different rate, there is no effect for the rate of deposition on the grain size value.

However, other works show that both of the materiel of substrate and deposition rate affect the grain size. Kirill and Horst [9] measured grain size of aluminum thin films with 100 nm film thickness deposited on different substrates and at different deposition rate using SEM as shown in table 1.3. Its clear that the values of grain size affected specially at high deposition rate.

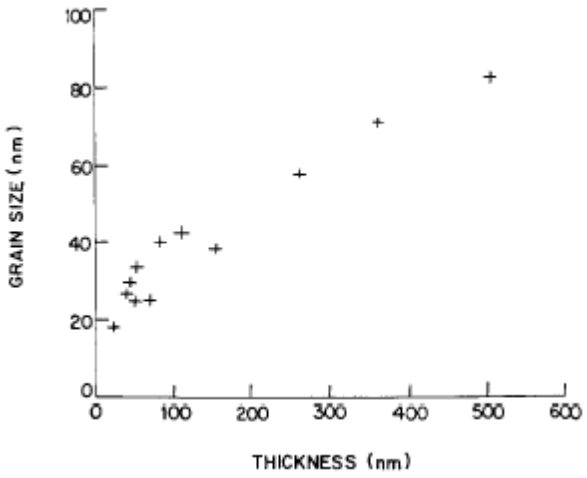

Figure 1.2: Grain size vs film thickness for aluminum film deposited on glass substrate [11]

Deposition rate, nm/s	Substrate		
	Glass	Silicon	Mica
0.1	20–40	15–30	15–30
0.2	20–40	15–40	15–30
0.5	20–50	20–40	20–40
1.0	30–70	20–70	30–70
2.0	40–100	30–80	40–100

Figure 1.3: Grain size (nm) for aluminum films deposited on different substrates at different deposition rate [9]

Grain size also can affect the reflection of light where as the grain boundaries increase the scattering increase and result in reduction in the total reflection as will be seen in this work. There are different methods used to measure the grain size of the material. One of the simplest way is drawing a random lines in SEM image and count the number of intercepts of grain boundaries and then divide it on total length of the drawn lines. This method is called "intercept method"[1]. In this method, more amount of efforts lead to high precision results.

1.3 Surface Roughness of Thin Film

Surface roughness or some times called roughness only, is a measurement of surface texture. It's a value represent the vertical deviations of a real surface from its ideal one. The surface considered as rough surface when these deviations are large and smooth in the opposite case. At nano scale and below, surface roughness play an important role in evaluating the performance of many devices such as micromirror. Building nano-devices require understanding and characterizing the nano-properties of material such as surface roughness [28].

Different factors affect the value of surface roughness of any material such as type of substrate and deposition rate. Kirill and Horst[9], measured the surface roughness of aluminum thin films (100 nm thick) deposited on different substrate and at different deposition rate as shown in figure 1.4. It's clear that both of these factors affect the value of the surface roughness where generally the roughness decrease as the deposition rate decrease. Also, each substrate results in different roughness values for aluminium films. As shown in figure 1.4, at higher deposition rate the value of roughness become higher in case of glass substrate and at the lower deposition rate the mica substrate gets lower value of roughness.

Surface roughness has an effect on reflection of the surface where as the roughness increase the reflection decrease. In the micromirror device, the reflection is specular reflection where the incident angle should equal to reflected angle to get optimum reflection. In the case of very smooth surface, the reflected wave is concentrated around the specular angle of reflection and that increase the reflection and the surface become mirror like. On the other hand, rough surface increase diffusion in the reflected light as a result of scattering and reduce the reflection of the material surface[2]

However, Makiko et al. [43] studied the effect of surface roughness on the reflection of aluminum at different wavelengths. They measured the reflectance for different aluminum alloys where their surface roughness range between 0.07 um and 0.86 um. They found that as the roughness of the surface increase the reflection also increase and there is no significant effect due to changing in wavelengths of the light. Also, as the value of the roughness decrease, the reflectance at the long side of wavelength is much decrease.

Surface roughness values are varying quantities and average value give best estimation. In mathematics, there is a statistical measurement used for varying quantities which is

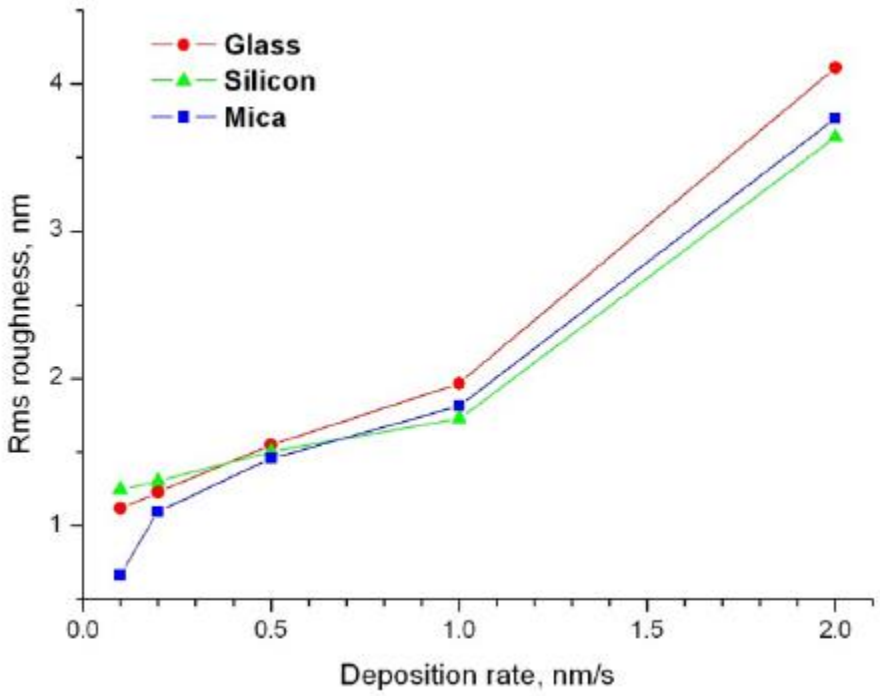

Figure 1.4: Surface roughness (RMS) for aluminum films evaporated on silicon, glass and mica substrates at different deposition rates[9]

called "Root Mean Square (RMS)" and described by equation 1.3

$$R_q = \sqrt{\frac{1}{n}\sum_{i=1}^{n} y_i^2} \tag{1.3}$$

Where: n is the number of values and y is the hight measured.

1.4 Elastic Modulus of Thin Film

Studying the reliability of the micromirror require investigating the elastic modulus property of the material used especially at Nano-scale where the properties is different from that in bulk materials. Metals, especially gold and aluminum, are mostly used in microomirror

device due to their high reflectivity. In metals, the heat and expansion are proportional to each other in which as the temperature of material increase, it will expand more. So, to get a high reliable mirror, i.e. avoiding failure, the value of elastic modulus should be optimum. Different factors cause variations in the value of elastic modulus for any material, such as type of the material, thickness of the film, temperature and method of fabrication. The thickness is the one that is more considerable where during the development of the micromirror device the overall size decrease and lead to decrease in the thickness of the film used in micromirror plate.

Many works have been done to measure elastic modulus of different materials at different thicknesses and different applications. Bharat and Vilas (1994) measured the hardness of the silicon (111) by a nanoindentation technique at depth of 1 nm for the first time using AFM where the reported depth of penetration at that time is 20nm [4]. They found that all of fabrication, film thickness and applied normal load affect the results of the hardness. Also, they investigated the value of nano-hardness and normal load as a function of penetration depth where the normal load increase as the depth increase and vice versa in the case of the nano-hardness. In their work, force-depth curve is used to determine the hardness as any other elastic or plastic properties and they suggested that it can be applied to a multilayered system. Another method used for measuring elastic modulus of thin film is self-deformed micromachining cantilever method that done by Weileun Fang in 1999 [16]. The author here determines the elastic modulus of the film through measuring the deflection of both the film and substrate due to residual stresses after fabrication. He derived an equation for a biaxial elastic modulus of the film as a function of radii of curvature, residual stresses and thicknesses of both the film and substrate and elastic modulus of substrate . He measured the elastic modulus of 0.1um and 0.3 um thick Si3N4 films that deposited on 1 um thick of SiO2 substrate. The elastic modulus of the film measured at different radius of curvature and he found that for a smaller film thickness, film's modulus does not influenced by radius of curvature of the film itself. However, the author concludes that this approach cannot be applied to a very thin film due to a difficulty in measuring the radius of curvature of the film.

In addition, the mechanical properties of a multilayered system was considered by measuring the nanomechanical properties such as elastic modulus and hardness for different multilayered system that interested in micromirror application such as digital micromirror devices [40]. Aluminum alloy (Al-Ti-Si) with 250 nm thick that deposited on silicon substrate has been studied and its elastic modulus and hardness at different contact depth was determined using nano-indentation method. At the contact depth of 30 nm, the hardness and elastic modulus are equal to 0.9 GPa and 91 GPa respectively. After that, as the contact depth increased, both of hardness and elastic modulus increased up to around 200

GPa for elastic modulus and 5 GPa for hardness at the depth of 500nm. Furthermore, after a comparison between a single and multilayered system, the author conclude that the value of hardness and elastic modulus of a multilayered is lower than in single layer system.

Atomic Force Microscopy can be used as a nano-indenter using a proper mode. Different modes can be applied in the AFM where they categorized into static and dynamic modes [22]. Essentially, AFM can work in three open loop modes which they are non-contact, contact and tapping mode [37, 6]. However, disconnecting the feedback loop, the mode will be changed to force spectroscopy mode that is straightforward way to extract elastic modulus [22]. Using force curve that resulted from force mode experiments, the nano-mechanical properties can be measured starting by calculate the slope of the unloading curve and using equations below to extract reduce modulus and from the reduced modulus calculate the elastic modulus of the film using a proper model [22].

Currently, and according to Nanoscope analysis software produced by Bruker [12], there are 2 different models deals with the force curve to extract mechanical properties such as modulus of elasticity. The first one is Hertz model (Spherical tip) that deal with rounded tip and use the equation 1.4 for elastic modulsu analysis.

$$F = \frac{4}{3}\frac{E}{1-\nu^2}\sqrt{R}\delta^{\frac{3}{4}} \tag{1.4}$$

where F = force (from force curve), E = Young's modulus (fit parameter), ν = Poisson's ratio (sample dependent, typically 0.2 - 0.5), R = radius of the indenter (tip) and δ = indentation

The other one is Sneddon model that deal with sharp and conical indenter as the case of this work and the equation of this model is as equation1.5 below where there is no dependency on the tip radius.

$$F = \frac{2}{\pi}\frac{E}{1-\nu^2}tan(\alpha)\delta^2 \tag{1.5}$$

where α = half-angle of the indenter In this work, nano-indentation experiment using AFM contact mode applied to determine the elastic modulus of aluminum thin films in the range of thicknesses between 10 and 125 nm to study the effect of film thickness on elastic modulus at very small scale size using Sneddon model that is used for sharp indenter tip.

Chapter 2

Methods

2.1 Reflectance Simulation using Opti-Wave tool

Opti-FDTD software package is used which is based on the finite-difference time-domain (FDTD) method. This method leads to an effective and powerful simulation analysis of nano device with ultra-fine structural details. In 2D simulation model, which is applied in this study, the system is laid on the Z-X axis where the propagation of the light is along the Z axis and Y axis is assumed to be infinite, figure 2.1. The observation line will detect the reflected light and for that purpose its position is behind the input field. In addition, the distance between the sample and the input field and between the sample and observation line are 100 nm and 150 nm, respectively, to be a far field simulation. In the input plane field, modulated continues Gaussian wave is used with input amplitude of 1 A/m. Anisotropic Perfectly Matched Layer (APML) boundary condition was used due to its high performance on simulation analysis [29].

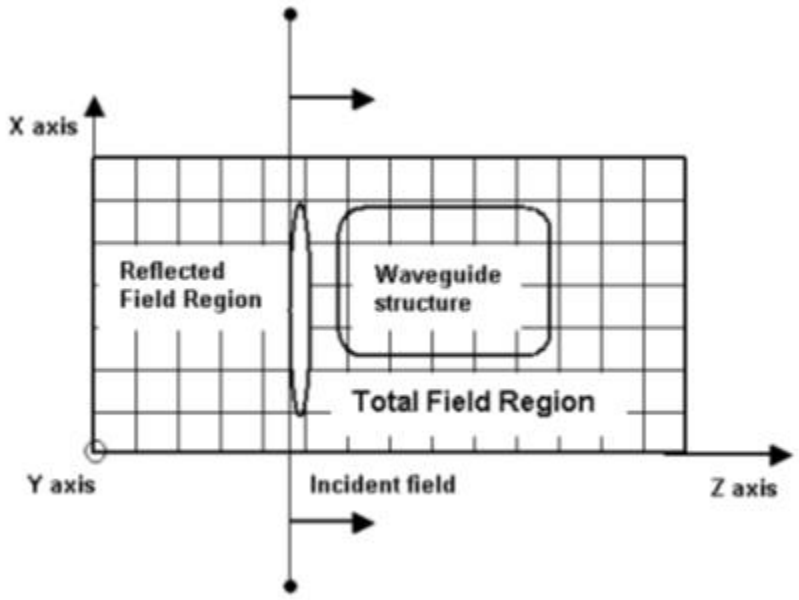

Figure 2.1: Schematic of 2D reflection simulation system[29]

2.2 Sample preparation

Single crystalline silicon wafers with (100) orientation were coated with 10,20,50,90,and125 nm thick aluminum films using Electron beam evaporation machine. In this process, as shown in figure 2.2, the chamber evacuated to 7.5x 10-5 Torr (10-4 hPa) to allow electrons to transfer from electron gun to the source material. Electron beams generated using thermal method. The accelerated electrons gain a high kinetic energy which will be converted to thermal energy after striking the source material. As a result, the source material (Aluminum) will be heated up to melting or sublimation point. At a sufficient level of temperature (room temperature) and vacuum (lower than 8E-6 Torr), vapor will result and then finally condense on the whole surface of the wafer [5]. The deposition rate was 0.5 A/sec and the error is 0.0001A.

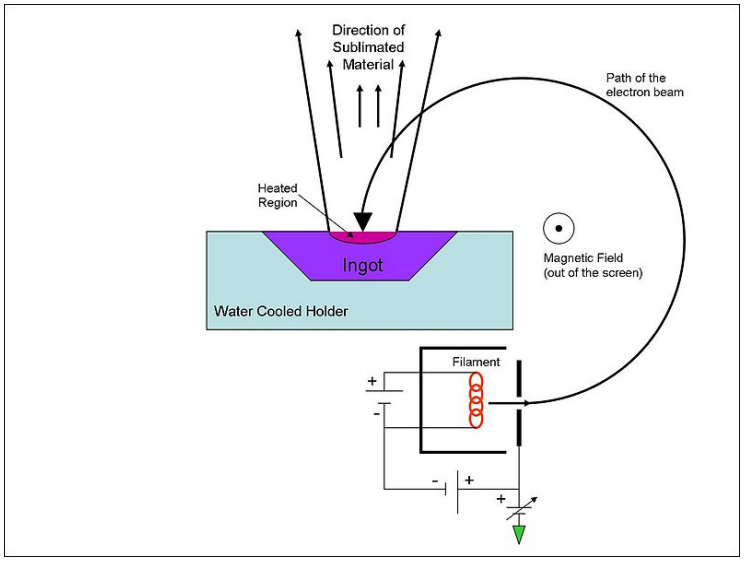

Figure 2.2: Schematic of deposition process using E beam evaporation method[5]

2.3 Reflection measurement

For measuring specular refection of the mirror, UV 2501PC spectrometer was used. This device operates under a double-beam system integrating sphere where at normal incident the sample beam enters the sphere and the reference beam enters at 8° angle of incident. Therefore, the specular reflection measurement is at incident angle of 8°. Furthermore, base line reflection measurement is required before measuring specular reflection of our sample. High reflective mirror should be used for base line reflection measurement and for that 300 nm silver film deposited on glass substrate was fabricated.

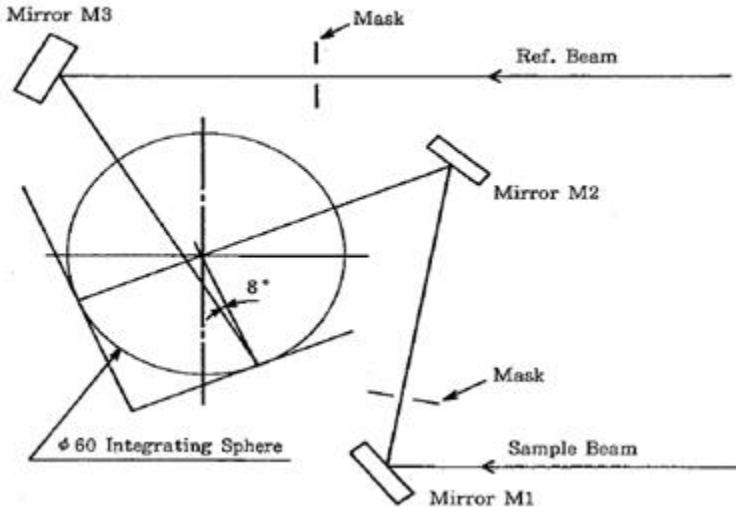

Figure 2.3: Schematic of operation principle and component of integrated sphere that used for specular reflection measurements

2.4 Grain size measurement using SEM

Grain size of the samples measured by applying average grain intercept method using Scanning Electron Microscopy (SEM). This method used to determine the average grain size which can be done by counting the number of intersections between the randomly drawn lines in different directions and grain boundaries to the total length of all drawn lines [1]. The image can be taken using SEM which is one of the most advanced electron microscopy that scan a focused beam of electrons to produce the image. Information of the surface topography of the sample obtained by detecting various signals resulted from the interaction of the electron and atoms of the sample. For some SEM, image can be achieved at very high resolution up to 1 nm. In brief, the operation of the SEM started by emitting electrons thermo-ironically from the electron gun where the electron beam that has an energy between 0.2 keV to 40 keV will be focused using one or two condenser lenses to a spot of about 0.4 to 5 nm in diameter as shown in figure 2.4 . After that, the beam go through pairs of deflected plates to deflect the beam in the x and y axes where then the scan will take place over a rectangular area of the sample surface to produce the image after interaction between the electrons and atoms of the sample [15]

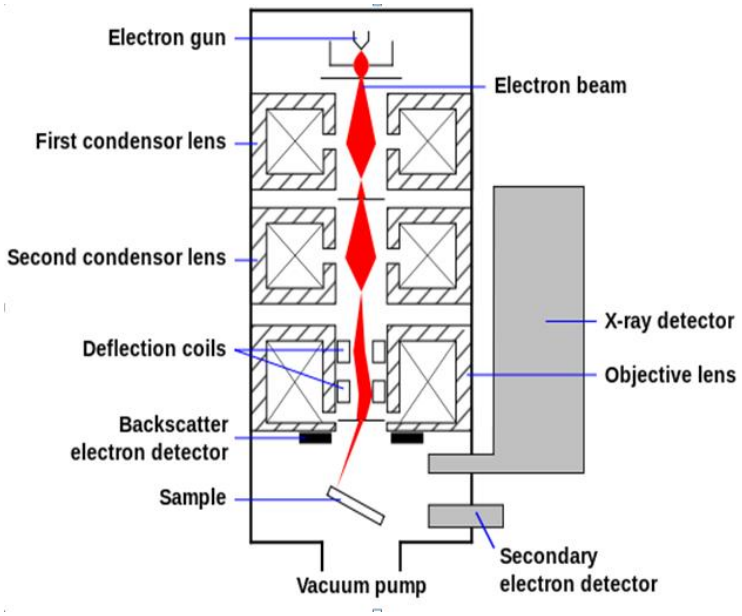

Figure 2.4: Main components of the SEM[15]

2.5 Surface roughness measurement using AFM (Tapping mode)

Atomic force microscopy (AFM) [3] is the most high resolution technique used for materials surface characterization. The relative movement between the sharp tip and the sample contain many data that can be used to extract surface and material properties. Figure 2.5 shows a schematic illustration of the AFM system components. By monitoring the displacement of the free end of the attached cantilever, the interaction between the tip and the sample surface can be measured and 3 different types of modes available which they are contact, non-contact and tapping mode.

In the tapping mode, during scanning the sample, the tip is oscillating around its resonance frequency and move towards the sample [7]. When the tip approach the sample surface, it only toughes or tapping the surface and that reduce the draging force which leads to reduce damage of the sample and this point is solving problem of contact mode [34]. A sensitive photo detector is used to receive a laser beam reflected from the back side of the beam to provide the value of cantilever deflection and then give a value of hight.

The Dimension 3100 Scanning Probe Microscope (SPM) using tapping mode was used

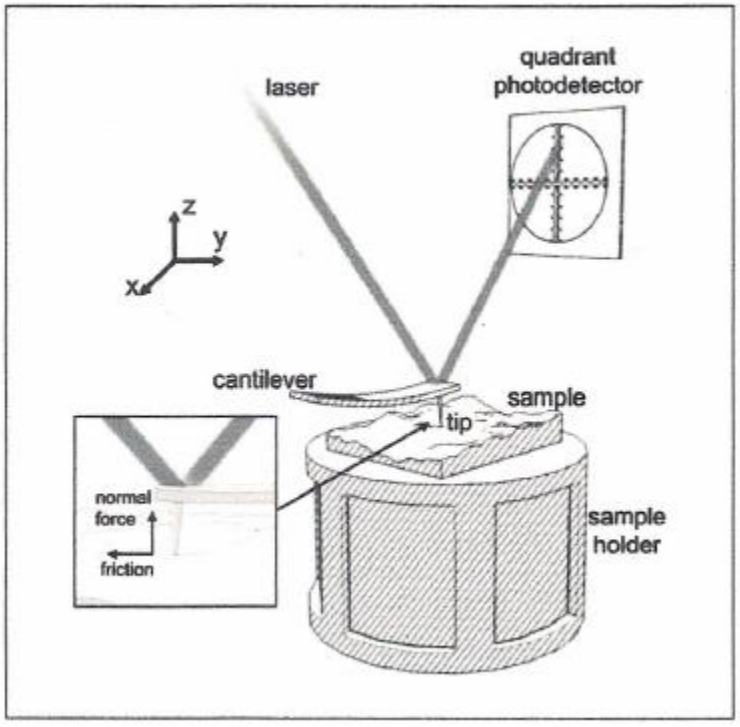

Figure 2.5: Simulation and experimental reflection results for different film thicknesses[31]

for measuring the surface roughness of the samples. 10um scan size was applied with 1:1 aspect ratio, 1.00 Hz scan rate and 256 samples per lines.

2.6 Elastic modulus measurment using AFM (Contact mode)

With too deep indentation depth, the mechanical properties of the film will be affected by substrate [39]. The rule of the thumb to avoid substrate effect is indent only tenth of the film thickness [20]. However, some times is difficult to be insure about the indentation depth or the device could not detect cantilever deflection at very low force, so, higher forces required but that will go to indent more than the tenth of the film thickness. for this case, a proper model need to apply to extract modulus of the film from the reduced modulus. Distortion in the force curve may take place due to sample roughness which affect the

indentation results of metals [33]. Rough surface cause a twist of the tip that resulted from the onset of the torsional momentum [30]. For a sharper tip with a radius 100 nm or less, the effect of the roughness on the indentation results is less sever [10]. Therefore, to overcome this issue, samples with very small roughness were prepared.

Normal elastic constant of the cantilever has to be measured and compared with the nominal value supplied by the producer, which is used to estimate the instantaneous applied load. Up to +/- 200 deviation from the nominal value is possible [18]. However, experimentally the elastic constant is measured. The values are very close to the nominal value, which is ranging from 228.4 N/m to 235.4 N/m at 300 nN trigger force. The lateral displacement has been neglected where the lateral elastic constant is usually much higher than normal one [18].

Basic operation of the AFM based on detection of attractive and/or repulsive surface forces [24]. This detection done by detecting the laser beam reflected form deflected beam. In the force measurement, at fixed position, the tip approach the surface and perform force-displacement analysis by applying force (cantilever deflection in z direction) and the corresponding displacement (penetration depth) would be recorded simultaneously and results in force curve [26]. From this curve a verity of mechanical properties can be extracted such as elastic modulus in this work.

After getting the force curve form the experiment, NanoScope Analysis software is produced by Bruker and used to analysis experimental data and get the required results such as elastic modulus in this work. One of its functions is indentation that can fit various indentation models to extract young's modulus using measured force curves. There are two models used in this software, Hertzian and Sneddon models. The first one is used for spherical tip shape while the Sneddon model used for conical tip shape as applied in this work.

Before starting indentation analysis, baseline correction should be done to measure the baseline tilt and offset and then applying linear correction to the whole force curve. This correction is used due to small amount of baseline tilt caused by detector configuration. This correction can be applied to one or both of extend or retract curves. Force is selected for Y axis and separation for X axis. After that the baseline correction source is selected for extend or retract curves.

Indentation analysis started by selecting one of the curves, extend(Loading) or retract(unloading) and the latest one is used due to high elasticity representation. There are two fit methods available in this program, contact point based and linearized methods. Contact point based can be applied to both indentation models where it uses a nonlinear least squares fit and goes through the contact point. The linearized method can be done

by takeing both sides of equations 1.4 and 1.5 to 1/2. The first one is used here where we can move the contact point to the depth where the elastic modulus be required to evaluate. At lowest separation, straight line is least squared-fitted to 5% of the points on the curve and then its slope is calculated. In case of using contact point fit method, there are two contact point algorithms. The first one is best estimate where the line that drawn between the first and last points is subtracted from each point in the force curve and the point with minimum value considered as contact point. Another algorithm is "treat as fit variable" where this algorithm used the contact point determined in best estimate method and then search points on increased separation up to 5% percent in z and compute its goodness of fit (R) for each point. After that, the contact point is selected where its the point with best goodness of fit.

Chapter 3

Results and Discussion

3.1 Simulation and Experimental reflection data

Figure 3.1 shows the simulation and experimental results of the reflection for different film thicknesses as a function of wavelength for aluminum films deposited on single crystal silicon (100). From the simulation results, it seems that as the thickness of the film increase the reflection increase. Also, except 10 nm film, as the wavelength increases the reflection decrease. At 10 nm film, the reflection is around 73% at lower wavelength (400 nm) and increases slightly up to 76% at higher wavelength (700 nm). However, at 20 nm thick film, it get higher reflection, 85%, and almost constant with changing the wavelength. Films with the thicknesses 50 and 90 nm yield similar reflection where they result in 90% reflection at 400 nm wavelength and decreased down to around 85% reflection at 700 nm wavelength. For the 125 nm thick film, the reflection also, decrease as the wavelength increase but it gets the highest reflection at lower wavelength (400nm), 92% and lower than 20, 50 and 90 nm thick films at higher wavelength(700 nm), 83%. In addition, there is a big jump between 10 and 20 nm thick films by around 10% of reflection.

Similarly, figure 3.1 shows the experiments results of the reflection of the thin films as a function of wavelength using UV 2501PC spectrometer. Similar to simulation results, as the film thickness increase the reflection value increase and as the wavelength increase the reflection value decrease except for the 125 nm thick film where its reflection increase as wavelength increase. 10 nm thick film gets the lowest reflection by 53% at 400 nm wavelength and decreased to around 46% at the higher end of the wavelength. The reflection increased by 10% at thickness of 20 nm and another 10% in the reflection increased at 50 nm thick film. For the 90 and 125 nm films, the reflection results in 85% at 400 nm

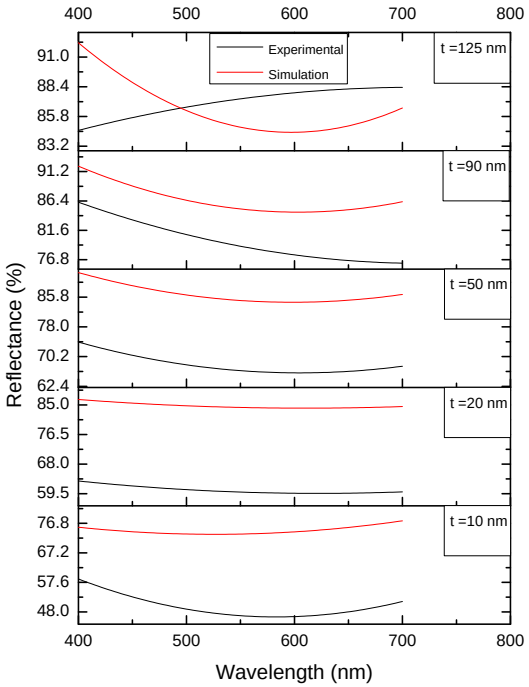

Figure 3.1: Simulation and experimental reflection results for different film thicknesses

wavelength and different values at 700 nm wavelength. Furthermore, comparing between the simulation and the experiments results for each film thickness show that as the film thickness decreases the deviation of experiments results from the simulation one increases.

According to simulation and experiments results, as the thin film increase, the reflection coefficient increase which is expected results. At 550 nm wavelength, the reflection of the films increased from 50% up to 85% between thicknesses of 10 and 125 nm. This result show that film thickness considered as one of the main factor to enhance photonic properties of the mirror. It seems from the results at lower wavelength (e.g. 400 nm)that the reflection is higher than at higher wavelength (e.g. 700 nm). That is because of the effect of refractive index. In this case, as the wavelength increase from 400 nm to 700 nm, the refractive index of aluminum film increase from 0.48787 to 1.92139 [27]. From the Fresnel equation at normal incident case, the reflection is inversely proportional to the addition of the reflective index of the two mediums [19]. Therefore, we expect lower reflection at higher wavelength more than at lower wavelength as we observed in our simulation and experimental results. Figure 3.1 also shows that as the film thickness decrease the deviation between simulation

and experimental results increase. For this observation, both of grain size and surface roughness were measured for all the films.

3.2 Grain size, surface roughness and reflectivity data

Using SEM images at very high magnification as shown in figure 3.2, were taken and random lines at different directions were also drawn to determine the average grain size using intercept method. Table 3.1 shows the results of grain size for different film thicknesses and details of calculation.

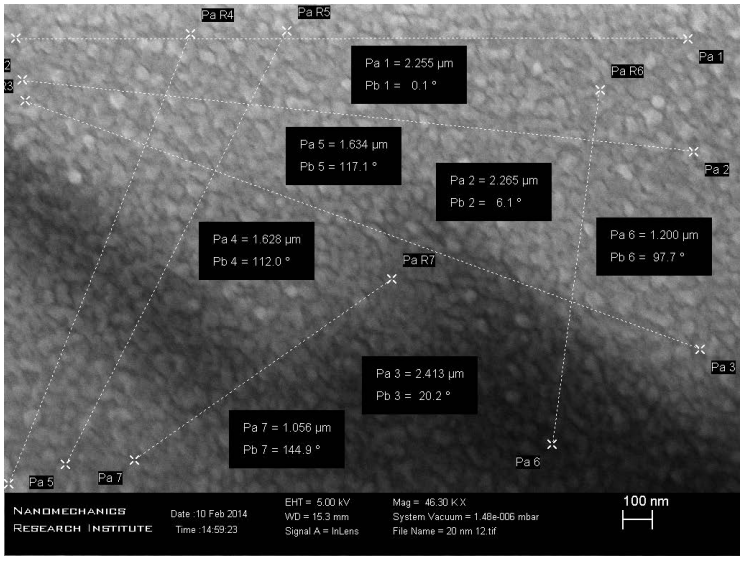

Figure 3.2: SEM image of 20 nm film thickness

Table 3.1: Average grain size for different film thicknesses

Film thickness (nm)	Total lines length (um)	Number of intercepts	Average grain size AGS (nm)
10	7.9983	185	43.2
20	12.45	273	45.6
50	7.3587	165	44.6
90	16.743	221	75.8
125	22.532	247	91.2

As in figure 3.4, it's clear that as the film thickness decrease the grain size decrease, too. That's lead to more grain boundaries and then increases the scattering of the reflected light and finally to reduction in the total reflection. Furthermore, figure 3.5 shows how the grain size has a significant effect on the reflectivity for different wavelengths.

Using tapping mode in AFM, the surface roughness of the samples determined using mean root square method where the probe scan the surface and average the heights it gets. The Dimension 3100 Scanning Probe Microscope (SPM) using tapping mode was used for measuring the surface roughness of the samples. 10um scan size was used with 1:1 aspect ratio, 1.00 Hz scan rate and 256 samples per lines. Table 3.2 shows the RMS roughness of the samples and figure 3.3 shows the results of the AFM for 10 nm film thickness sample.

Table 3.2: Surface roughness RMS for different FIlm thicknesses

Film Thickness (nm)	10	20	50	90	125
Surface roughness RMS (nm)	0.937	2.370	2.353	2.847	2.071

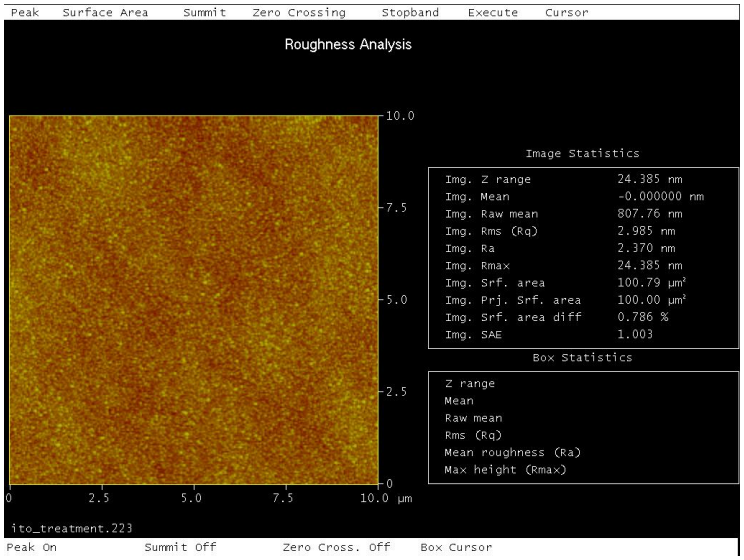

Figure 3.3: AFM results of 20 nm film thickness

Similarly for grain size, as the film thickness increases the roughness increase except for the higher thickness (125 nm). Increase in the surface roughness is due to enlarge of the mountains, valleys and island as a result of aggregation of the native grains into the larger cluster [23]. However, as the film thickness increase the roughness decrease as happened at

125 nm film which is become smoother due to decreasing of the influence of the substrate [41]

Figure 3.4 shows the effect of film thickness on surface topography properties. It indicates that as the film thickness increase both of the grain size and surface roughness increase except for the 125 nm film where there is a drop in the surface roughness value. In addition, grain size and roughness have an effect on the reflection of the film as shown in figure 3.5 and 3.6 where it tells that there is an almost linear proportionality between grain size and roughness of the films and their reflection values at different wavelengths.

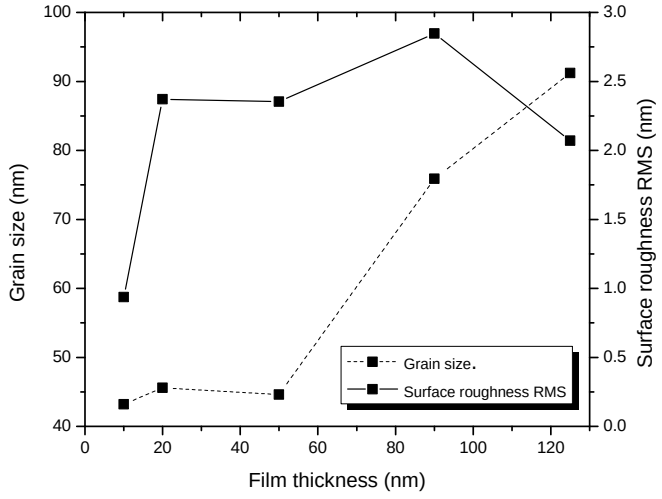

Figure 3.4: Grain size and surface roughness for different Al film thicknesses

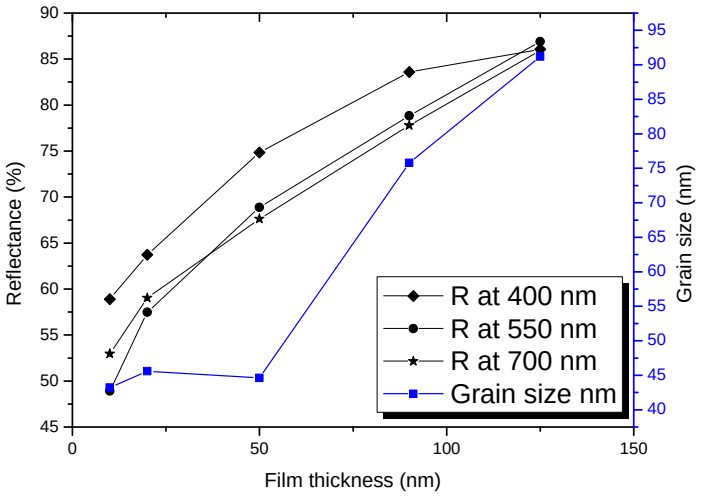

Figure 3.5: Effect of grain size on reflection values for different Al film thicknesses

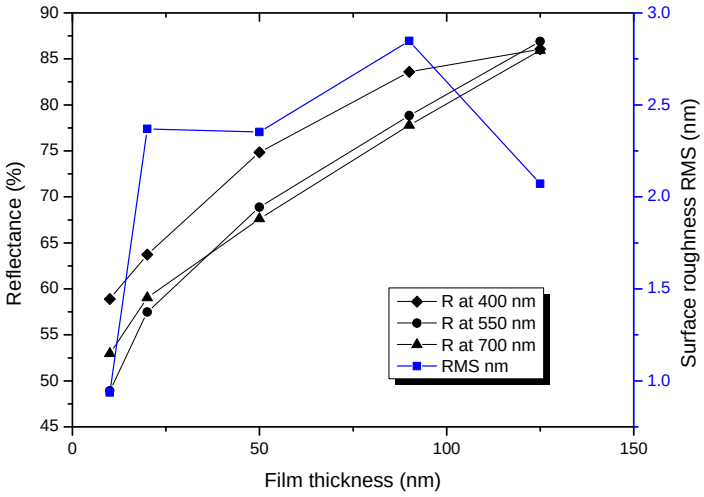

Figure 3.6: Effect of surface roughness on reflection values for different Al film thicknesses

3.3 Elastic Modulus Data

Elastic modulus of the film done by performing 3 nano-indentation experiments per each sample and analysis all of them and then averaging the results to get optimum results. Using Nanoscope Analysis 1.5 software allow us to get the values of elastic modulus of the samples at any depth as shown in figure 3.7 where it shows the sample modulus vs applied force. It's clear that as applied force increase (deeper depth), the elastic modulus increase and that is due to substrate effect [36, 35, 10].

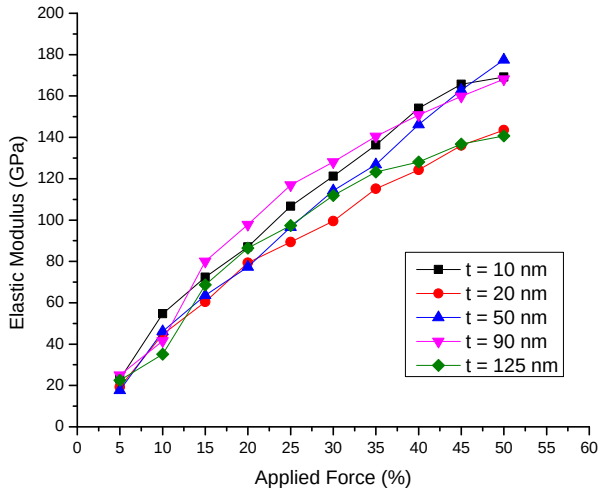

Figure 3.7: Results of Elastic modulus for all films as a function of applied force

One of the approach used in literature to extract the elastic modulus of the film is 10% rule of thumb [36, 10]. This rule states that until the tenth of film thickness, the value of modulus represent for the film only and after that the substrate effect is started affect the modulus value. However, according to Agilent Technologies [35], this rule does not work for elastic modulus. They measured elastic modulus of gold(1.5 um thick) and they found that the sample modulus increase contiguously after 1% of the film thickness. That indicates that the substrate effect start early before 10% of the film thickness and it requires another approach to extract film modulus. Similar to the results in this work and as shown in figure 3.8 , the modulus of the sample increase immediately as the force applied which confirms that 10% rule of thumb does not work for elastic modulus.

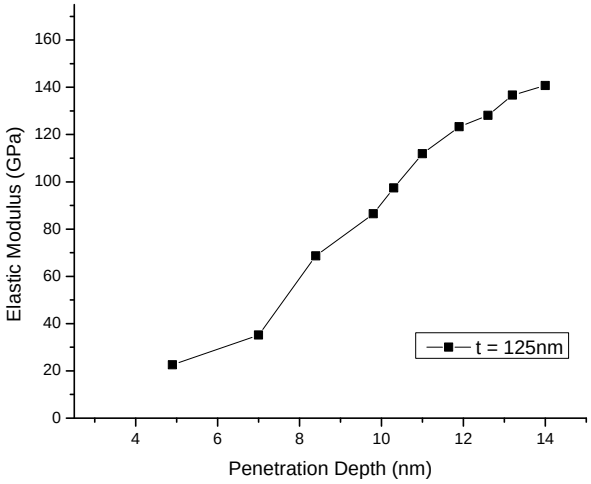

Figure 3.8: Results of elastic modulus of 125 nm film thick to show the 10% rule of thumb

Another approach to extract film modulus from the combined one is plotting measured elastic modulus at different penetration depths vs a/t ratio and after that, fitting the the data to get optimum curve and extrapolated it to zero a/t (a is contact radius, t is film thickness)[10]. The point behind this way is that at zero a/t, the tip of the indenter is almost at the top of the surface of the film and that gives best representation of film modulus. However, this way is applied in this work but it gives very strange results as shown in figure 3.9 , where at zero a/t ratio the value is very low and come in negative value. May that due to the difficulty to give precise calculation for the contact radius due to very sharp tip which it requires a different work to develop a proper model that can work with it.

Rather than 10% rule of thumb or a/t ratio, simpler way can be used to extract film modulus which is extrapolate the fitted cuve of E vs. F to zero applied force. As mentioned, sample modulus can be determined at any penetration depth and from figure 3.7 it seems that as depth increase the value of modulus increase due to substrate effect. That's mean at initial applied force the modulus value give best results for the film where the tip is at the surface for the film as shown in figure 3.10 where it tells that the film modulus = 72 GPa and that give good agreement with bulk value.

From figure 3.7, after 50% of applied force the value of the sample modulus become close to substrate value and because of that determining of film modulus does not include

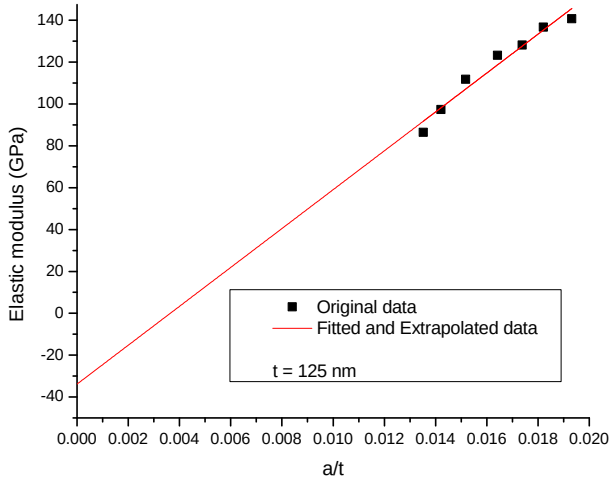

Figure 3.9: Results of elastic modulus as a function of a/t ratio for 125 nm film thick

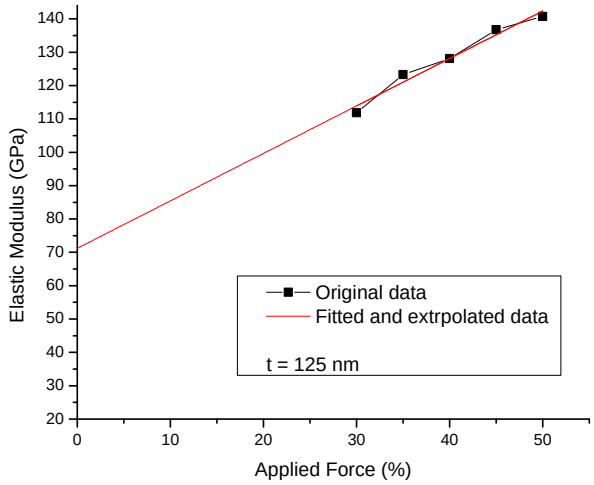

Figure 3.10: Film's modulus result using extrapolating the fitted curve to zero applied force

the data after that where the substrate effect will increase. Also, at the beginning of the indentation, roughness of the surface and error in initial penetration depth will results in very small value where avoiding them will increase the reliability of the final results. Between 20 and 50 % of the applied force, the sample elastic modulus increase almost linearly with the applied force and linear fitting and extrapolating to zero applied force is used for analyzing the data.

Figure 3.11 shows the final results of elastic modulus as a function of film modulus. As the film thickness decrease the film modulus decrease slightly at 125 and 90 nm film thickness compared to bulk value. However, at 50 and 20 nm film thickness, there is a big drop in the modulus value of the film where they result in 17 GPa and 40 GPa, respectively. After that, the film's elastic modulus goes up again up to 49.7 GPa at 10 nm film thickness.

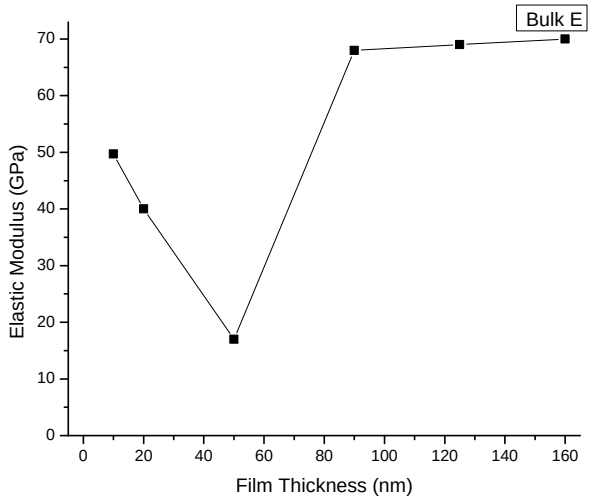

Figure 3.11: Final results of film's modulus as a function of film thickness

Chapter 4

Conclusion

To sum up, the effect of film thickness at ultra-thin film size on the optical reflection and elastic modulus of mirror was studied using Si(100) substrates coated with aluminum films. We have demonstrated how the film thickness affect the reflection of light and elastic modulus. Both of simulation and experimental works of mirror reflection verify that as the film thickness decrease the reflection of the mirror decrease up to very low reflection at very thin film, 10 nm. Also, increase in the deviation between the simulation and experiment results as the film thickness decrease was observed. The reason behind the deviation between the simulation and experimental results was observed after studying the surface topography of the films, grain size and surface roughness. Decreasing in the grain size as the film thickness decrease illustrate the reason of increasing in the deviation between the simulation and experimental results. In addition to that, even the roughness affect the reflection value, but here is show that no significant effect and that due to very low roughness value (1 - 3 nm). Similarly, film thickness affect the elastic modulus of the film. As film thickness decrease, the film modulus decrease slightly at 125 nm and 90 nm thick films and their values are close to the bulk one. At 50 nm, the modulus of the film decrease sharply down to 17 GPa and then goes up to 49.7 GPa at 10 nm thick film.

.

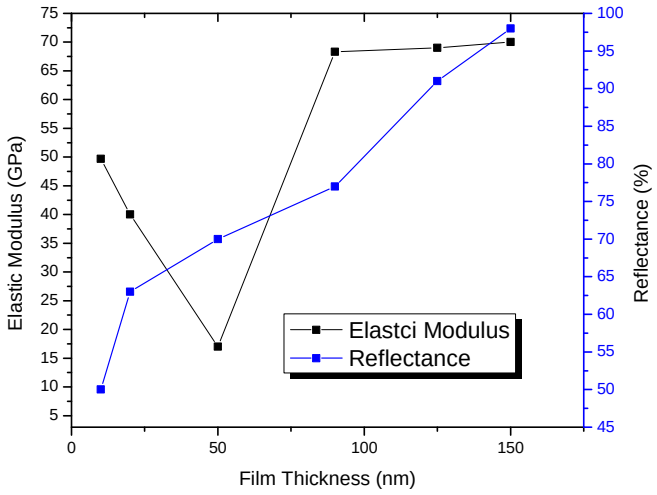

Figure 4.1: Effect of film thickness on reflection and elastic modulus compared to bulk value

Chapter 5

Further Research

Surface topography affect the reflection of the mirror as concluded from this study. Therefore, optimizing the surface topography such as increase the grain size of very thin film will results in higher reflection. So, it recommended to perform a study to minimize the grain size effect considering the deposition method and substrate effects.

In addition, from the results of film modulus, there is a sharp decrease at 20 nm and 50 nm thick films. It recommended to do a similar study at 15, 30, 40 nm thick films to verify this decreasing. Also, developing a new model to extract the film's modulus from the combined one will increase the reliability and precision of the elastic modulus results.

APPENDICES

5.1 Thin Films Reflection Results

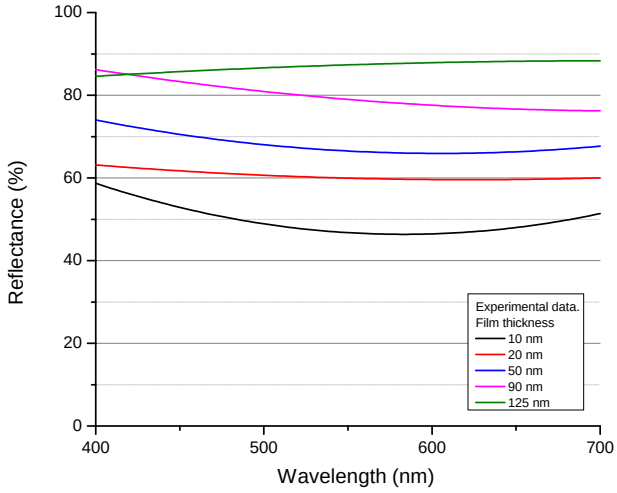

Figure 5.1: Experimental reflection results for different films thicknesses

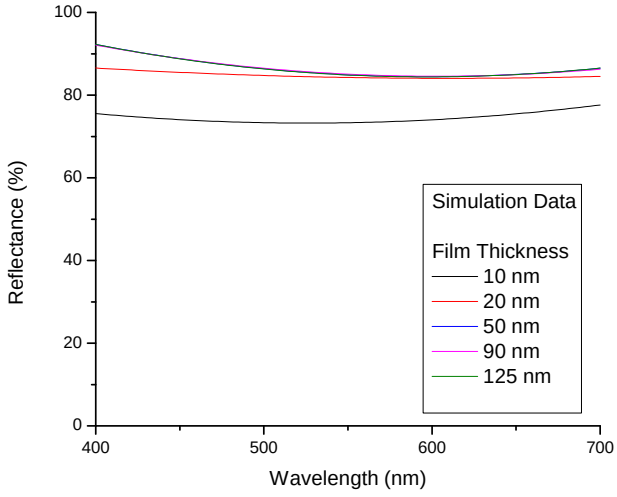

Figure 5.2: Simulation reflection results for different films thicknesses

5.2 Elastic Modulus of Thin Films

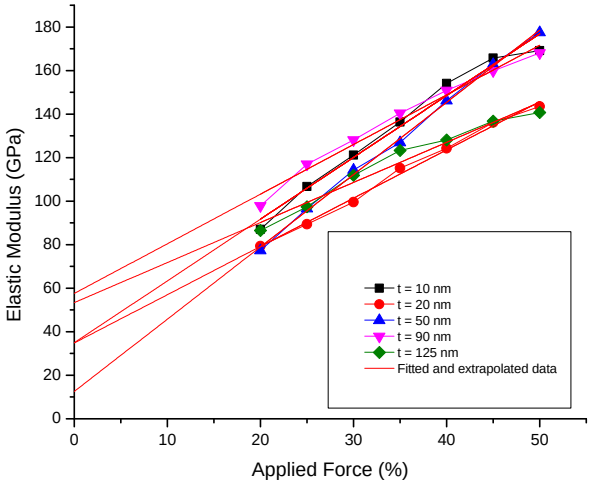

Figure 5.3: Elastic modulus results of films by extrapolating starting by 20% of applied force

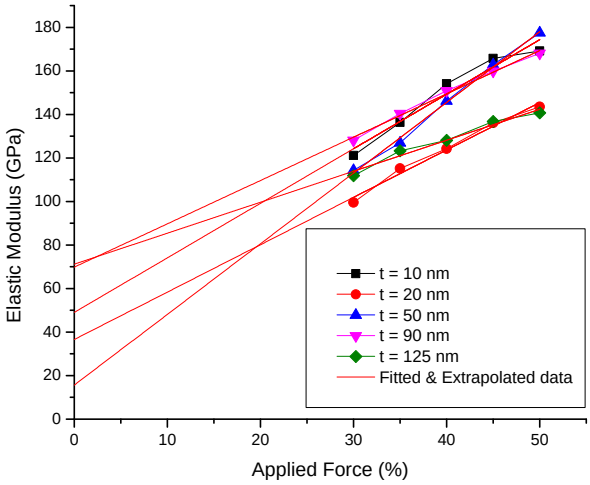

Figure 5.4: Elastic modulus results of films by extrapolating starting by 30% of applied force

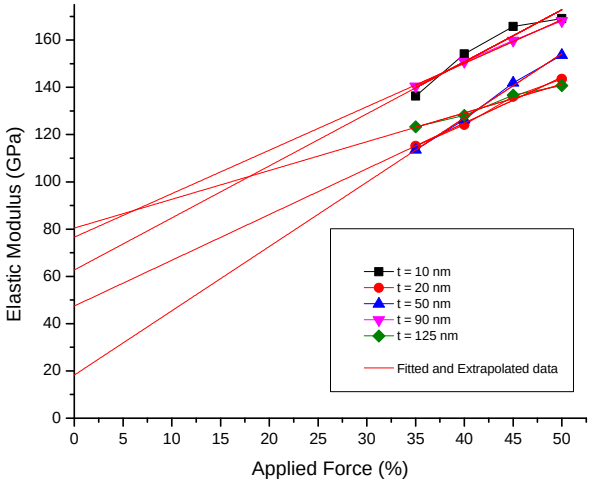

Figure 5.5: Elastic modulus results of films by extrapolating starting by 35% of applied force

5.3 AFM results for surface roughness measurment

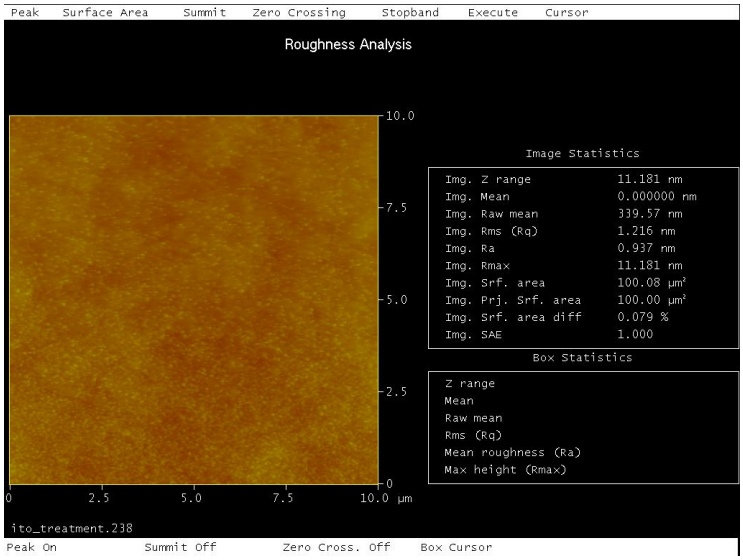

Figure 5.6: AFM results of 10 nm film thickness

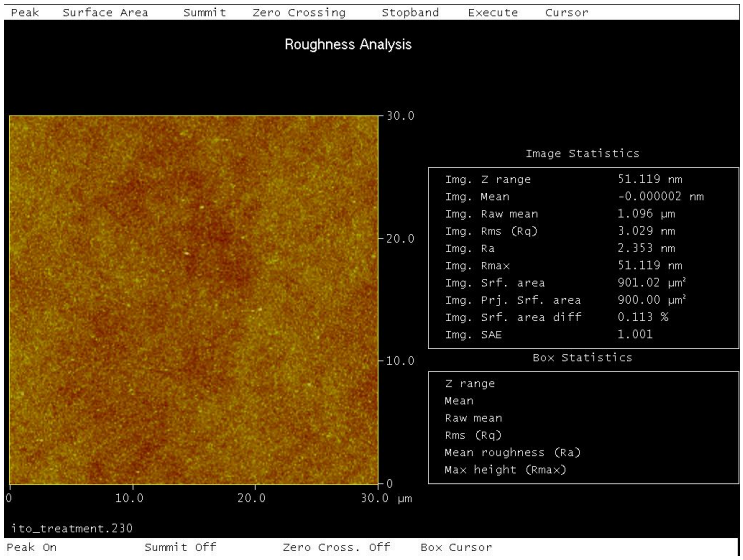

Figure 5.7: AFM results of 50 nm film thickness

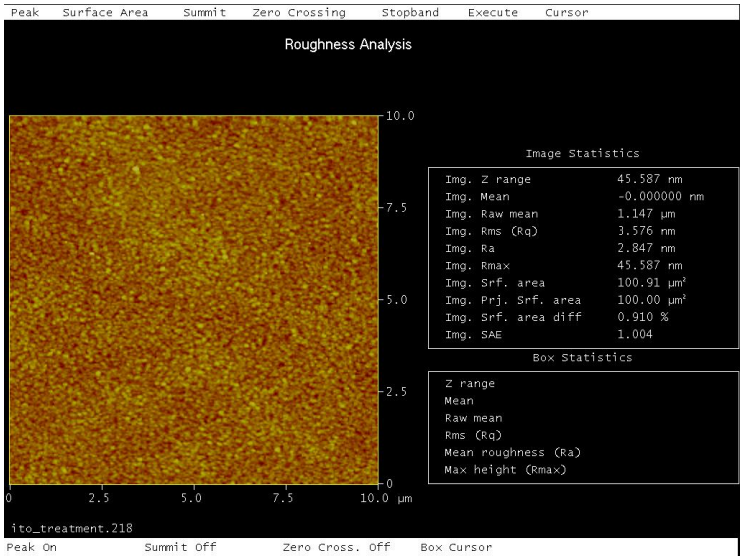

Figure 5.8: AFM results of 90 nm film thickness

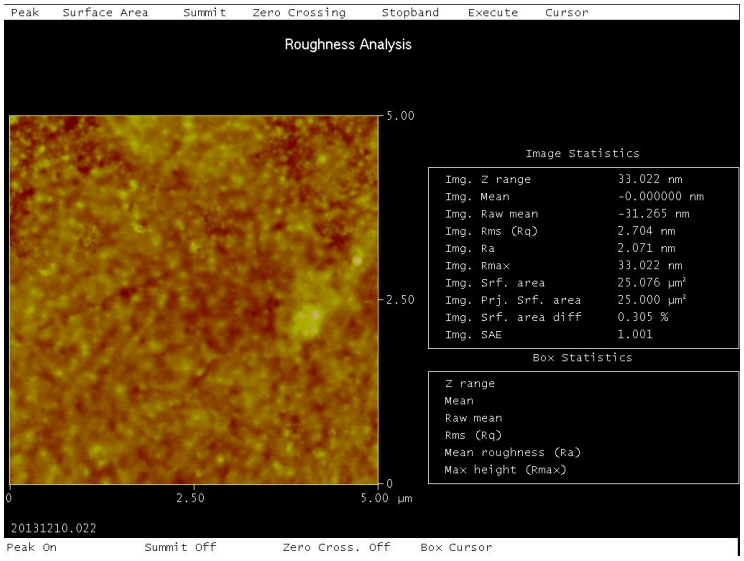

Figure 5.9: AFM results of 125 nm film thickness

5.4 SEM images showing grain size measurements

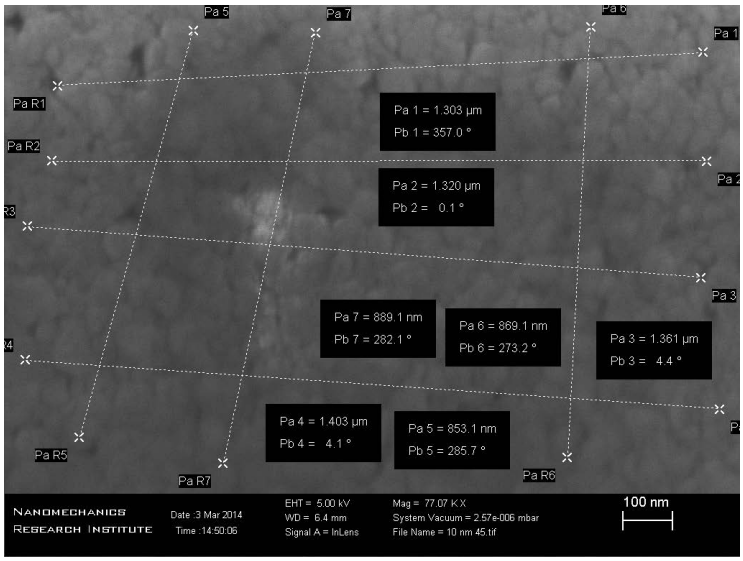

Figure 5.10: SEM image of 10 nm film thickness

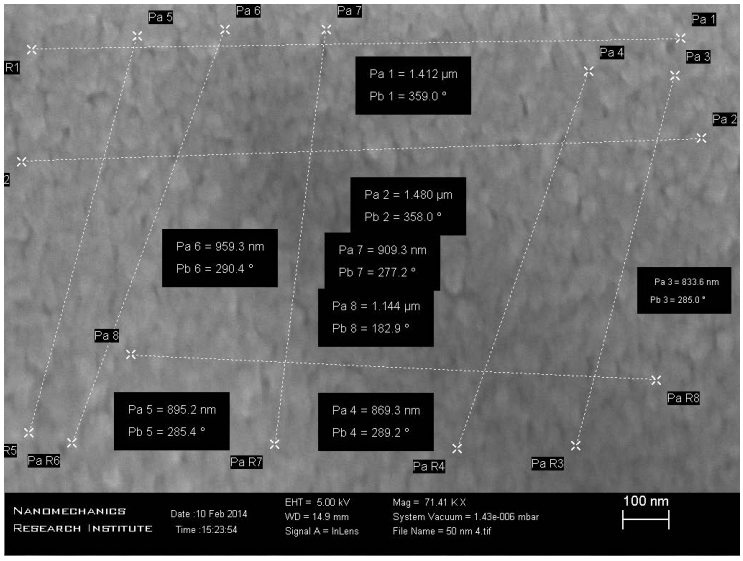

Figure 5.11: SEM image of 50 nm film thickness

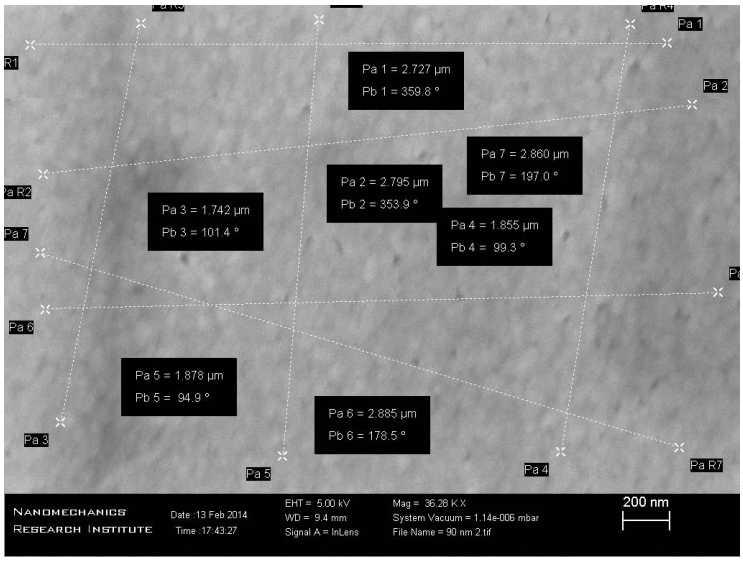

Figure 5.12: SEM image of 90 nm film thickness

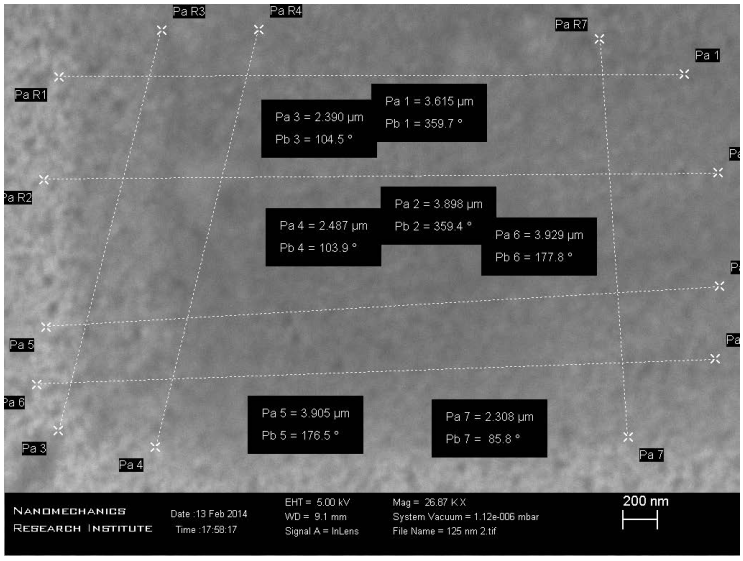

Figure 5.13: SEM image of 125 nm film thickness

References

[1] ASTM E112 13. Standard test methods for determining average grain size, November 2013,URL:http://www.astm.org/Standards/E112.htm.

[2] AluMatter. Effect of surface roughness on reflectivityonline, September 2013. URL: http://www.aluminium.matter.org/.

[3] AZoNano. Fundamentals of contact mode and tappingmode atomic force microscopy, 2014. URL:http://www.azonano.com/article.aspx?ArticleID=3010.

[4] B. Bahrat and N. Vilas. Nanoindentation hardness measurments using atomic force microscopy. *Applied physics Let.*

[5] Electron beam physical vapor deposition, January 2014. URL: http://en.wikipedia.org/.

[6] M. Bezanilla, B. Drake, and E. Nudler. Motion and enzymatic degradation of dna in the atomic force microscop. *J Biophys.*

[7] C. Binnig, G. Quate, and C.F. Gerber. Atomic force microscope. *Phys. Rev. Lett*, 56:930933, 1986.

[8] K. Bordo. Effect of deposition rate on structure and surface morphology of thin evaporated al films on dielectrics and semiconductors. *Material Science*, 18, 2012.

[9] K. Bordo and H. Rubahn. Effect of deposition rate on structure and surface morphology of thin evaporated al films on dielectrics and semiconductors. *MATERIALS SCIENCE*, 4.

[10] Anthony C. and Ficher-Chripps. *Nanoindentation.* Springer, 2011.

[11] D. Chaverri, A. Saenz, and V. Castano. Grain size and electrical resistivity measurements on aluminum polycrystalline thin films. *Materials Letters 12*, pages 344–348, 1991.

[12] Bruker Company. Nanoscope analysis1.50 manual. pages 244–251.

[13] CorrsionPedia. Grin boundaries, February 2014. URL:http://www.corrosionpedia.com/definition/599/grain-boundary-gb.

[14] K. Du, X. Pang, C. Chen, and A. A. Volinsky. Mechanical properties of evaporated gold films. hard substrate effect correction. *Materials Research Society*.

[15] Scanning electron microscope, September 2013 URL:http://www.en.wikipedia.org/.

[16] Weileun Fang. Determination of the elastic modulus of thin film materials using self-deformed micromachined cantilevers. *J. Micromech. Microeng*.

[17] G. Hass and J. E. Waylonis. Optical constant and reflectance and transmittance of evaporated aluminum in the visible and ultraviolet. *Journal of the optical Society of America*, 51:7, 1961.

[18] J.L. Hazel and V.V. Tsukruk. *Thin Solid Films*, 339:249, 1999.

[19] O. S. heavens. *Optical properties of thin solid films*. Dover Publications, INC, 1955.

[20] C.H. Hsue and P. Miranda. *J. Mater. Res.*, 19:94, 2004.

[21] V.P. Jaecklin, C. Linder, J. Brugger, N.F. de Rooij, J.-M. Moret, and R. Vuilleumier. Mechanical and optical properties of surface micromachined torsional mirrors in silicon, polysilicon and aluminum. *Sensors and atom A*, 43, 1994.

[22] J. Diaz F. Sanz J.J. Roa, G. Oncins and M. Segarra. Calculation of youngs modulus value by means of afm. *Bentham Science Publishers Ltd*.

[23] E. Karimazadeh, A. Arman, B. Astinchap, A. Ahmadpourian, B. Safibonab, and A. Boochani. Investigation fractal and thickness effect on oxidize layer behavior of cu thin films by afm. *European Journal of Scientific Reseach*, 111:491–499, 2013.

[24] T.G. Kuznetsova, M.N. Starodubtseva, N.I. Yegorenkov, S.A. Chizhik, and R.I. Zhdanov. Atomic force microscopy probing of cell elasticity. *Micron*, 38(8):824–833, 2007.

[25] Braggs Law, September 2013. URL: http://en.wikipedia.org/.

[26] H. Liu. Mechanical characterization of aortic valve interstitial cells and their nuclei using atomic force microscopy. *Master thesis, Department of Mechanical and Industrial Engineering, University of Toronto*, pages 13–18, 2012.

[27] M. I. Markovic and A. D. Rakic. Determination of the reflection coefficient of laser light of wavelengths (0.22 m , 200 m) from the surface of aluminum using the lorentz-drude model. *Optical Society of America*, 29:24, 1990.

[28] Asylum Research AFM models. Measuring surface roughness with atomic force microscopy, 2014. URL:http://www.asylumresearch.com/Applications/SurfaceRoughness/SurfaceRoughness.shtml.

[29] OptiWave. *OptiFDTD Users Reference*. OptiWave, support@optiwave.com, version 10 edition, 2011.

[30] J.R. Pratt, D.T. Smith, D.B. Newell, J. Kramar, and E. Whitenton. *J. Mater. Res*, 19:366, 2004.

[31] J.J. Roa, G Oncins, J. Diaz, F. Sanz, and M. Segarra. Calculation of young modulus value by means of afm. *Reasrch patents in Nanotechnology*, 5:27–36, 2011.

[32] J.E. Steinwall and H. H. Johnson. Mechanical properties of thin film aluminum fibers: Grain size effects. *Materials Research Society*, 188.

[33] D. Tabor. The hardness of metals. *Clarendon Press, Oxford*, 1951.

[34] R. Tamayo and J. Garcia. Deformation, contact time, and phase-contrast in tapping mode scanning force microscopy. *Langmuir*, 2:44304435, 1996.

[35] Agilent Technologies. Indentation rules of thumb , applications and limits. 2010.

[36] D. Tranchida, Z. Kiflie, and S. Piccarolo. Atomic force microscope nannoindentation to reliably measure the young's modulus of soft matter. *Modern Research and Educational Topics in Microscopy*, 2007.

[37] Ukraintsev VA. Rocking y-shaped probe for critical dimension atomic force microscopy. *US20090100917*.

[38] K.W. Vogt, P.A. Kohl, W.B. Carter, R.A. Bell, and L.A. Bottomle. Characterization of thin titanium oxide adhesion layer on gold: Resistivity, morphology and composition. *Surface Science*, 1993.

[39] N.E. Waters and Br. *J. Appl. Phys.*, 16:557, 1965.

[40] G. Wei, B. Bhushan, and S.J. Jacobs. Nanomechanical charachterization of mutilayered thin film structures for digital micromirror devices. *Ultramicroscopy.*

[41] Jijiun Yang, Youlan Huang, and Kewei Xu. *Surface and Coating Technology 201*, 2007.

[42] Zhimin J. Yao* and Noel C. MacDonald. Single crystal silicon supported thin film micromirrors for optical applications. *Cornell University School of Electrical Engineering and Cornell Nanofabrication Facility*, 1997.

[43] M. Yonehara, T. Matsui, K. Kihara, H. Isono, A. Kijima, and T. Sugibayashi. Experimental relationships between surface roughness, glossiness and color of chromatic colored metals. *Materials Transactions*, 45:1027–1032, 2004.